Microchimica Acta (2018) 185: 101
https://doi.org/10.1007/s00604-017-2615-3

ORIGINAL PAPER

Graphitic carbon nitride nanosheets as a fluorescent probe for chromium speciation

Nadereh Rahbar[1,2] · Zeinab Salehnezhad[3] · Amir Hatamie[4] · Ahmad Babapour[2]

Received: 31 August 2017 / Accepted: 9 December 2017 / Published online: 10 January 2018

Abstract

A fluorometric method was developed for simultaneous determination of Cr(VI) and Cr(III) ions using graphitic carbon nitride nanosheets (g-C_3N_4 NS) as a nanosized fluorescent indicator probe. The g-C_3N_4 NS were prepared using high-temperature carbonization of melamine followed by ultrasonication-assisted liquid exfoliation. The g-C_3N_4 NS display fluorescence with excitation/emission peaks located at 320 and 450 nm. The chromium speciation is based on the quenching of g-C_3N_4 NS fluorescence. The total concentration of chromium is determined after oxidation of Cr(III) to Cr(VI). The Cr(III) content was then calculated by subtracting the concentration of Cr(VI) from that of total chromium. The effects of pH value, probe amount, and contact time are optimized. Under optimum conditions, calibration plots are linear in the range in the 0.01 to 100 μM chromium concentration range. The limit of detection is 3 nM for for Cr(VI). The intra- and inter-day relative standard deviations (RSD) of the assay are 3.6–7.5% and 4.1–8.5%, respectively. The indicator probe was applied to the determination of chromium species in spiked water and food samples, and recoveries were satisfactory (93.9–107.0%).

Keywords G-C_3N_4 nanosheets · Nano fluorophore · Melamine · Carbonization · Photoluminescence · Quenching · Transmission electron microscopy · Atomic force microscopy · X-ray powder diffraction · Stern-Volmer plot

Introduction

Cr(VI) presents higher toxicity to living organisms with mutagenic, carcinogenic, and teratogenicity potentials than Cr(III) which is a necessary nutrient and has a significant task in transferring sugar, proteins, and lipid [1]. Owing to significant differences in the biochemical properties of Chromium species there is an obvious need for their accurate quantification separately. The assessment of chromium risks and toxicity in various environmental and food matrices requires effective speciation studies by determining the concentrations of Cr(III) and Cr(VI) separately rather than the total chromium content alone.

Many efforts have been made for chromium speciation in various matrices. The use of sensitive and selective analytical technique such as atomic absorption spectrometry (AAS) [2], inductively coupled plasma-atomic emission spectrometry (ICP-AES) [3], inductively coupled plasma-mass spectrometry (ICP-MS) [4, 5], ion chromatography (IC) [6], and high performance liquid chromatography (HPLC) with ICP-MS detector [7] coupled with a prior separation, extraction and/or preconcentration steps, is a common strategy to simultaneously monitor Cr(III) and Cr(VI) in a matrix. Thus, various pretreatment methodologies such as dispersive liquid–liquid micro extraction (DLLME) [8], hollow fiber liquid phase micro extraction

Electronic supplementary material The online version of this article (https://doi.org/10.1007/s00604-017-2615-3) contains supplementary material, which is available to authorized users.

✉ Nadereh Rahbar
n_rahbar2010@ajums.ac.ir; n_rahbar2001@yahoo.com

✉ Amir Hatamie
amirhatchem@yahoo.com

[1] Nanotechnology Research Center, Ahvaz Jundishapur University of Medical Sciences, Ahvaz, Iran

[2] Department of Medicinal Chemistry, School of Pharmacy, Ahvaz Jundishapur University of Medical Sciences, Golestan road, Ahvaz 6135733184, Iran

[3] Student Research Committee, Ahvaz Jundishapur University of Medical Sciences, Ahvaz, Iran

[4] Department of Materials Science and Engineering, Sharif University of Technology, Azadi Avenue, Tehran 11155-9466, Iran

(HF-LPME) [9], solidified floating organic drop micro extraction (SF-ODME) [10], cloud point extraction (CPE) [11], and solid phase extraction (SPE) [12] have been developed. However, these analytical methods using expensive and sophisticated instrumentation coupled with pretreatment or sample preparation processes in some cases usually are time consuming and trained experts are needed to run these procedures. In addition, simple spectrophotometric and spectrofluorimetric methods have been employed in chromium speciation analysis, though they suffer long sample preparation procedures and/or low sensitivity [13–17].

Among the commonly used analytical methods, the fluorimetric method, which is based on fluorescence quenching, is one of the most successful approaches used to detect and quantify of various metal ions. On the other hand, the selectivity and sensitivity of general analytical methods have been remarkably enhanced by introducing different nanostructures such as nanoparticles, quantum dots, and nanosheets. A number of fluorescent-probes have been reported for chromium detection based on these nanostructures [18–20].

Today, g-C_3N_4 NS has attracted considerable attention because of its nontoxic characteristics, high thermal and chemical stability with good electrical and optical properties. Bulk g-C_3N_4 as metal-free semiconductor (with a band gap of ~2.6 eV), is the most stable allotrope among different carbon nitride materials comprising two-dimensional (2D) frameworks of tri-s-triazine connected via tertiary amines (Fig. S1) [21]. Generally, g-C_3N_4 NS can simply be prepared by carbonization of nitrogen-rich precursors such as melamine, thiourea and urea and exfoliating them to convert compact layers of bulk g-C_3N_4 to many thin layers (nanosheets) with nanometer thickness (−). Compared to 2D g-C_3N_4 NS with atomic-scale thickness, when compared with bulk g-C_3N_4, has large surface area which contains many active coordination sites (lone-pair electrons of nitrogen atoms) with a strong photoluminescence (PL) activity [22]. The use of these nano-structures as nano-fluorophore have been reported in determining some analytes such as Cu^{2+} [23], Cr(VI) [24],, nitro aromatic explosives [25], riboflavin in milk and drink [26], DNA [27], and cytochrome C [28].

The main aim of this study was to develope a simple, fast and green method for chromium speciation using g-C_3N_4 NS as label-free fluorescent probe based on significant fluorescence quenching - by Cr(VI). Up to our knowledge, this is the first time that spectrofluorimetry method is being used for the analysis of chromium species in food and water real samples using a nano-fluorophore. The ultrathin g-C_3N_4 NS was synthesized using simple thermal pyrolysis of melamine and liquid exfoliation in water, and the various analytical parameters affecting the performance of nano-fluoroprobe were optimized in speciation procedure.

Experimental

Materials and apparatus

All chemicals were obtained from Merck (Darmstadt, Germany www.merckgroup.com) except melamine that was purchased from Samchun Chemicals Co. (Korea www.samchun.com). All solutions were prepared using deionized water. Cr(III), Cr(VI), and Ce(VI) stock solutions were prepared by dissolving the appropriate amounts of $Cr(NO_3)_3.9H_2O$, K_2CrO_4 and $Ce(SO_4).4H_2O$ in deionized water. In preparation of Ce(IV) solution 0.5 mL of H_2SO_4 (96%) per 50 mL solution was used. Tris-HCl and phosphate buffers (pH 7) were prepared using the standard procedure. All aqueous solutions were prepared using deionized water and all the experiments were performed at ambient temperature. The spectrofluorimetric measurements were carried out using Termo SCIENTIFIC–LUMINA (America) fluorescence spectrometer. UV–Vis spectrum of the g-C_3N_4 NS was recorded on a Shimadzu model UV-1650PC UV-Visible spectrophotometer (Japan http://www.ssi.shimadzu.com). Fourier transform infrared (FT-IR) spectra were recorded using a Bomem MB series instrument (Quebec, Canada www.bomem.com). Transmission electron microscopy (TEM) images were collected using a Zeiss EM900 (Germany www.zeiss.com) instrument. An atomic force microscopy (AFM) instrument was used to show the dimensions and morphology of the g-C_3N_4 NS (Nanowizard II, Germany www.jpk.com). X-ray powder diffraction (XRD) results were collected by using a Bruker D8-FOCUS diffractometer (www.brukersupport.com). Zeta-potential results were obtained with the help of a zeta-sizer (Malvern Instruments, U.K. ww.malvern.com). ETHOS1 microwave digestion system was used for real sample preparations (Milestone, Italy www.milestonesrl.com). The phase separation of the sample solution was performed on CLEMENTS laboratory centrifuge (Sydney). The pH values were controlled using a Metrohm pH-meter model 623 (Herisau, Switzerland www.metrohm.com). Liquid exfoliation of g-C_3N_4 was performed using an ultrasonic bath (Elma, Germany www.elma-ultrasonic.com).

Preparation of ultrathin g-C_3N_4 NS

The bulk g-C_3N_4 was prepared by direct pyrolysis of melamine in the semiclosed system. Typically, 5 g of melamine was heated at a rate of 3-°C min^{-1} and 600-°C for 4 h in a porcelain crucible. The light yellow solid product was the bulk g-C_3N_4 (Fig. S2). To obtain ultrathin g-C_3N_4 NS, a liquid exfoliating method was used. For this purpose, 50 mg of the bulk g-C_3N_4 powder was dispersed in 50 mL deionized water followed by ultra sonication for about 16 h to obtain a light yellow dispersion. The suspension was centrifuged at

5000 rpm for 5 min to remove large-sized nanosheets or the residual unexfoliated g-C_3N_4. It is important to mention that the monolayer g-C_3N_4 material with highly water-dispersity was stable in 4 °C for at least 6 months without any depositing or color changes. In order to identify the structure and morphology of synthesized g-C_3N_4 NS, XRD, TEM, IR, and AFM techniques were employed.

PL sensing procedure

A simplified schematic illustration of the analytical procedure is shown in Fig. 1. In order to detect Cr(VI) with the optimized procedure, 5 μL of the prepared g-C_3N_4 NS dispersion was mixed with a 1 mL Tris-HCl buffer (0.1 mol.L^{-1}, pH 7) in a 10 mL volumetric flask containing different concentrations of Cr(VI). Then, the solution was diluted to the mark with deionized water and was incubated for 5 min at room temperature. The PL emissions of the solutions were recorded at 320 nm excitation and 450 emission wavelengths. To determine the total chromium concentration, before the addition of g-C_3N_4 NS, 0.6 mL Ce(IV) solution (1000 mg.L^{-1}) as oxidizing reagent was added to the solution containing chromium species to convert Cr(III) to Cr(VI) (Fig. S3). After allowing the solution to stand for 5 min, its total chromium content was determined using the aforementioned method. The Cr(III) content was calculated by subtracting the Cr(VI) concentration from the total chromium concentration. A blank solution was also run under the same conditions without adding the analyte and the analytical data were obtained based on fluorescence intensity difference between blank and sample solutions (F_0-F). All the experiments were performed in triplicate.

Sample preparation

Water samples were collected from two sources: [1] tap water which provides drinking water for Ahvaz without any treatment and [2] Karoon River water which supplies water to Ahvaz with subsequent filtration using suitable membrane. The water samples were directly analyzed. All food samples were acquired from local shops. For garlic and onion samples 2 g of fresh samples were cut, crushed, and homogenized thoroughly and transferred to microwave vessels. Then, HNO_3 (8 mL, 65%) and 4 mL of H_2O_2 (30%) were added to each vessel and the vessels were allowed to react for approximately 2 min before sealing the vessels. Thereafter, the vessels were heated at 150 °C (900 W) for 20 min in a microwave system. Microwave digestion procedure for real milk sample was similar to the aforementioned method except for the fact that 6 mL of the milk was mixed with 4 mL of HNO_3 (65%). All the digested samples were transferred into the 25 mL volumetric flasks and were diluted to the mark with deionized water after adjusting their pH at 7. The blank solutions were prepared under the same conditions without food samples.

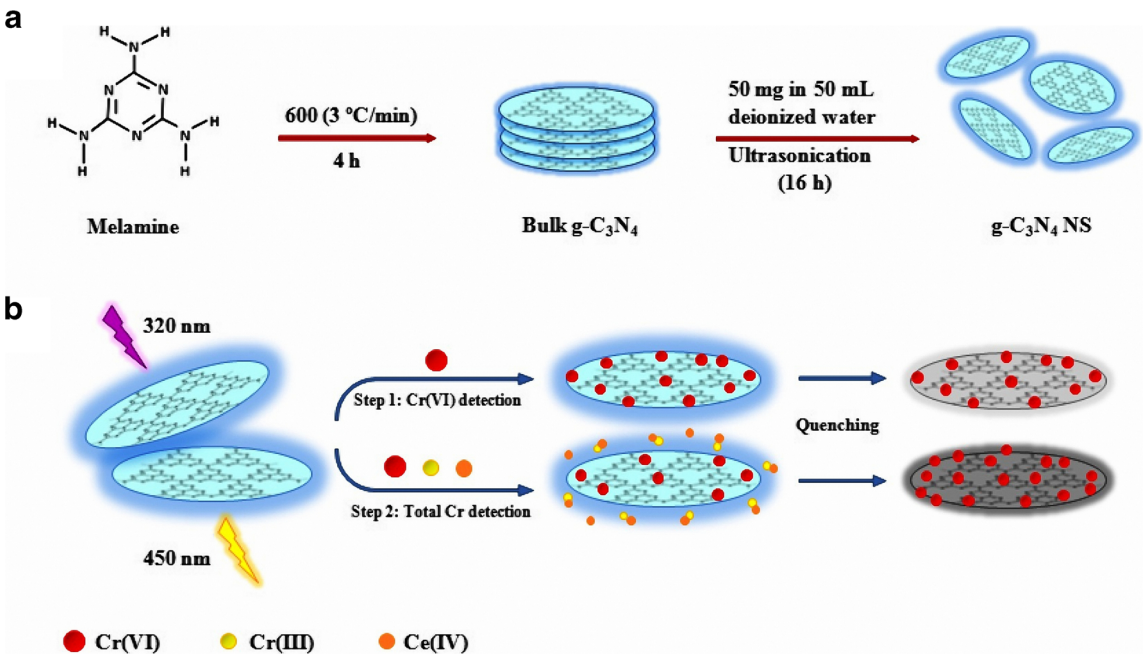

Fig. 1 Schematic illustrationof (**a**) synthesis of bulk g-C_3N_4 by carbonization of melamine and exfoliated g-C_3N_4 NS by the use of ultrasonication, and (**b**) an analytical pathway for simultaneous determination of Cr(VI) and Cr(III) based on fluorescence quenching mechanism in two steps: 1) quenching of g-C_3N_4 NS fluorescence intensity by Cr(VI) and 2) conversion of Cr(III) content of the sample solution to Cr(VI) via oxidation by Ce(IV) ions and detection of total chromium

Results and discussion

Spectroscopic properties of g-C_3N_4 NS

The optical properties of g-C_3N_4 NS were investigated using UV-visible absorption and emission spectra. The UV-visible absorption and PL spectra exhibited two absorption bands located at 226 and 316 nm and a fluorescence peak at 450 nm for the nanosheets, respectively (Fig. S4). The maximum PL intensity was achieved at an excitation wavelength of 320 nm which was almost consistent with the peak at 316 nm in its UV-Vis spectrum (Fig. S5). In addition, only one PL peak at a wavelength of 450 nm was obtained with the excitation wavelengths changing from 300 to 370 nm, suggesting the location of emission peak for g-C_3N_4 NS was excitation-independent and the nanosheets included only a single emitter [24]. The prepared g-C_3N_4 NS dispersion was found to be stable for at least 6 months without the observations of any floating or precipitated particles. The photograph of the g-C_3N_4 NS dispersion under day-light, UV light and laser light (showing the occurrence of the Tyndall effect and the colloidal nature of the dispersion) is shown in the inset of Fig. S4.

The quenching mechanism

As suggested in previous reports, sp^2 C − N in conjugated tris-triazine rings is responsible for intrinsic fluorescence of bulk g-C_3N_4 through the electronic transition between n nonbonding (HOMO) and π antibonding orbitals (LUMO) [29]. On the other hand, it might be assumed that Cr(VI) can bind to the nitrogen atoms via its free electron pairs on the surface of the nanosheets through hydrogen bond, and such bonding brings g-C_3N_4 NS and Cr(VI) into close proximity with each other. Afterwards, photo-induced electron transfer (PET) from the excited states (LUMO) of g-C_3N_4 NS to the d orbitals of Cr(VI) can be occurred as a result of its severe electron deficiency, and as such a considerable decrease is observed in PL intensity of the emitter [30]. Another possible quenching mechanism can be described in the context of inner filter effect (IFE). In this mechanism, the good spectral overlap between excitation and/or emission wavelengths of a PL emitter and the absorption band of a quencher is necessary [24]. As mentioned earlier in this study, an excitation wavelength of 320 nm which is almost consistent with the maximum adsorption wavelength of as prepared g-C_3N_4 NS at 316 nm, can provide adequate energy for electronic transition creating subsequent PL with maximum intensity. In addition,The UV-Vis spectrum of Cr(VI) solution with two intense and well defined adsorption peaks at 272 and 370 nm, and also one weak peak 413 nm, possesses adequate overlapping areas with absorption and emission spectra of g-C_3N_4 NS (Fig. S4A) [14]. Therefore, the dramatic decrease in PL intensity of the nanofluorophore can be attributed to the obvious absorption of the exciting radiation at 320 nm (PL excitation wavelength of g-C_3N_4 NS) by Cr(VI) and as a consequence quenching phenomenon is occurred.

Characterization of g-C_3N_4 NS

Figure 2a presents the typical FT-IR spectra of both bulk and nanosheets of g-C_3N_4. The absorption band at 812 cm^{-1} originates from the vibration of triazine rings, indicating the existence of the units with NH and NH_2 groups. In this structure, the peaks in the region from 1200 to 1800 cm^{-1} can be attributed to stretching modes of either trigonal C − N(−C) − C or bridging C − NH − C units in g-C_3N_4. Peaks between 3000 and 3600 cm^{-1} corresponded with N − H and O − H stretching and hydrogen-bonding interactions. XRD technique was used to determine the crystalline features of the synthesized materials. The XRD patterns of bulk and nanosheets of g-C_3N_4 are shown separately in Fig. 2b.Two pronounced diffraction peaks were found at about 13.0° and 27.0° for bulk and nanosheets of g-C_3N_4. The distinct peak at 13.0° (100) can be attributed to in-planar structural packing of tri-s-triazine units. The second and sharper peak at 27.0° (002) corresponds to the characteristic interlayer stacking peak of the conjugated aromatic systems in g-C_3N_4 which is indexed for graphitic materials. Fig. 2c shows a TEM image of g-C_3N_4 NS. As it can be seen from this figure, the nanosheets have a two-dimensional structure and its surface morphology is layered as in the case of graphite. AFM observations were also conducted to verify the successful exfoliation of bulk g-C_3N_4, as shown in Fig. 2d. The AFM images of g-C_3N_4 NS show a thickness ranging from 1.5 to 4 nm, revealing that the g-C_3N_4 NS included less than 12 C − N (inset figure) [31].

Optimization of sensing conditions

In order to obtain better performance of the method, several related conditions were evaluated including pH, type and concentration of buffer, amount of nano-fluoroprobe, incubation time, and amount of oxidant were evaluated. Respective data and Figures are given in the Electronic Supporting Material. The best experimental conditions were found to be as follows: a) a sample pH value of 7 (Fig. S7A); (b) a g-C_3N_4 NS dispersion volume of 5 μL (Fig. S7B); (c) a reaction time of 10 min (Fig. S7C).

Analytical performance and method validation

Several analytical parameters for quantitative analysis such as LOD, LOQ, linear dynamic range (LDR), accuracy and precision under optimized conditions were studied. With the increase of Cr(VI) concentrations at ten selected levels (in each linear region) in the range of 0.01–100 μM (~ 0.52–5200 μg L^{-1}), the PL intensity of the solution containing appropriate

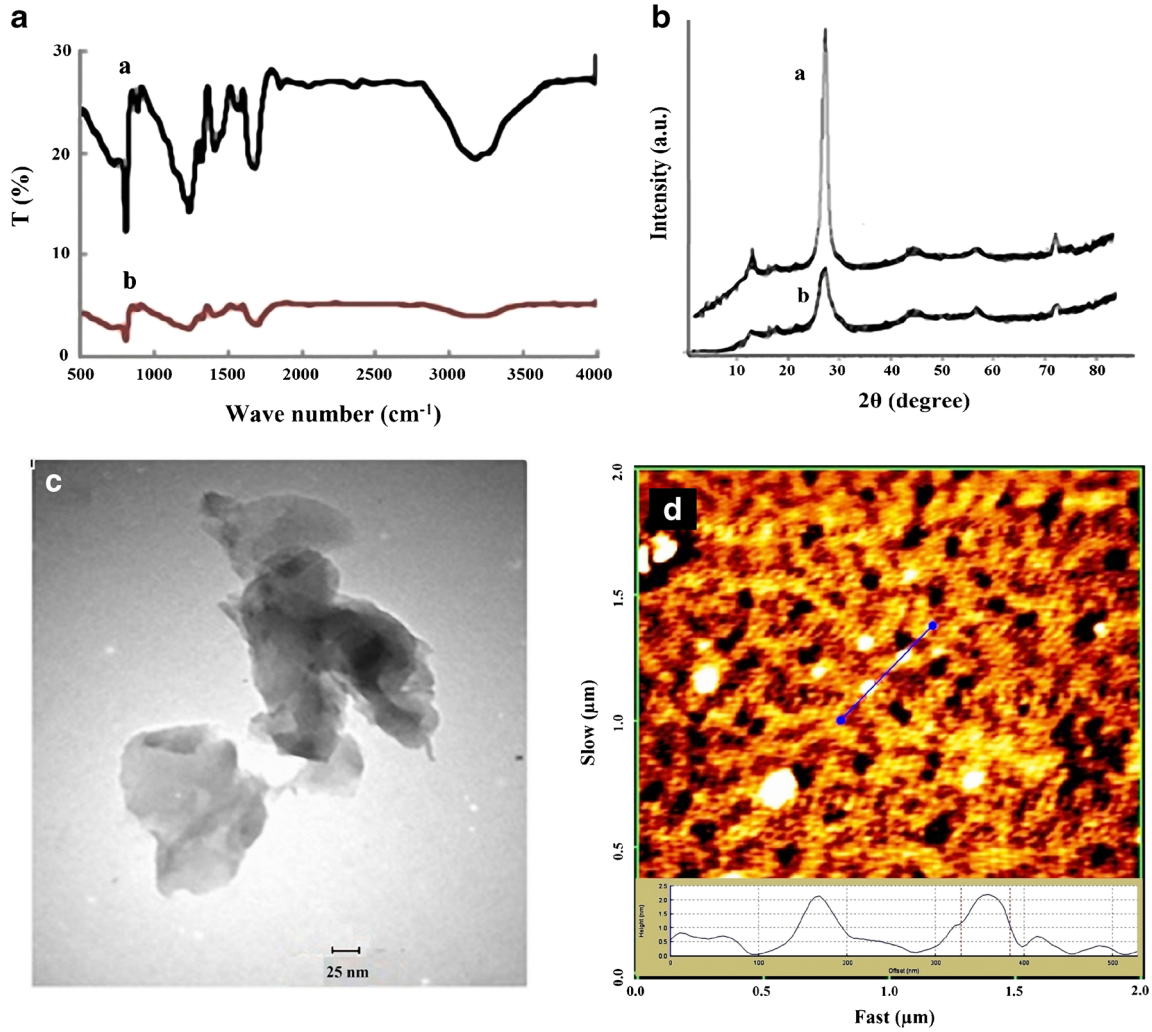

Fig. 2 **a** FT-IR spectrum; **b** XRD pattern; **c** TEM image, and **d** AFM topography of g-C_3N_4 NS (inset: the height of nanosheets)

amount of g-C_3N_4 NS was decreased and the calculated F_0-F term was increased linearly. All the data were the averages of three determinations and the calibration curve was constructed using least squares linear regression method. Two calibration curves were obtained for determination of Cr(VI) ion in the ranges of 0.01–0.25 and 0.50–100 μM (Fig. 3). The LOD and LOQ of the method for Cr(VI) based on three and ten times the standard deviation rule for the blank (3 and 10 Sb/m) were 0.003 and 0.01 μM ($n = 10$), respectively. The equations for the calibration graphs and other analytical features of the method are presented in Table S1. The F_0-F measurement for analyte solution containing the quality control (QC) amount of Cr(VI) was interpolated from the calibration curve on the same day to give concentration of the analyte. To evaluate the intra- and inter-day precision and accuracy data showing the reproducibility and repeatability terms, five similar experiments were carried out for the QC samples at concentration levels of 0.25, 1 and 25 μM on the same day and on three consecutive days. As shown in Table 1, the RSD% results range from 3.6 to 7.5% and 4.1 to 8.5% for analysis of intra-day and inter-day spiked samples, respectively, revealing the suitable reproducibility of the method. The analytical performance of the current method and the other previously reported techniques for the speciation of chromium ions are compared in Table 2. In general, the methods which are coupled with an extraction and preconcentration process, present lower LODs than the other techniques; however, this step is more intricate and time consuming. In comparison with the other existing fluorescent methods, the g-C_3N_4 NS based assay shows improved LOD value and is quite rapid to perform. In addition, this method presents widest linear range among all the analytical techniques.

The quenching effect of a quencher can be quantitatively determined by Stern–Volmer equation: $F_0/F = 1 + K_{SV}[Q]$ where F_0 and F are the PL intensities in the absence and presence of quencher ions, K_{SV} is the Stern–Volmer constant and [Q] is molar concentration of the quencher [30]. A plot of F_0/F versus [Q] (1–50 μM) for Cr(VI)-g-C_3N_4 NS system showes linear dependency with regression coefficient (R^2) and slope (K_{SV}) values of 0.9985 and 1.96×10^4 M^{-1},

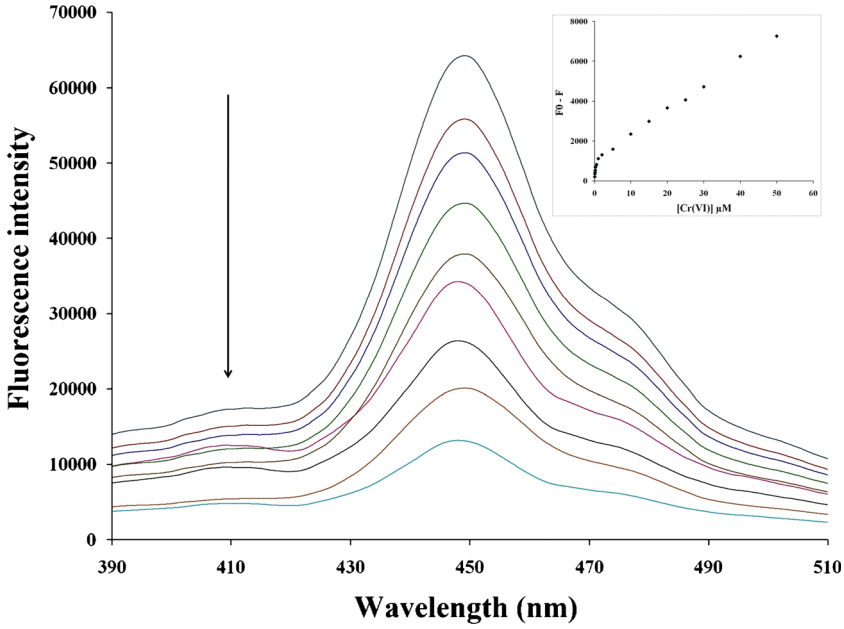

Fig. 3 The Cr(VI) concentration-dependent fluorescence responses profiles. The inset is the calibration curves in the concentration rage of 0.01–100 μM

respectively (Fig. S9). This large K_{SV} value together with low LOD (0.01 μM) of the method indicated that Cr(VI) has the strong quenching effect on the PL intensity of g-C_3N_4 NS.

Interferences study

To explore the selectivity of g-C_3N_4 NS to the Cr(VI), the influence of some potentially interfering substances including various cations (200 μM) on the quenching ability of 50 μM Cr(VI) were examined using the optimized method. The tolerance limit was considered as the concentration of the added species causing less than 5.0% relative error. Based on the results illustrated in Fig. 4, some of the examined cations, namely Cu^{2+}, Hg^{2+} and Fe^{3+}, caused a slight decrease in PL intensity. However, they did not seriously affect the PL intensity in the presence of Cr(VI). Anyway, owing to the chemical feature of Cr(VI) as anion, the interference effects of these cations were successfully eliminated by addition of EDTA as a masking agent and good selectivity was achieved for the method. In addition, in order to eliminate the potential interferences in real samples, the standard addition method was used for analysis of the analyte.

Application of the method to water and food samples

In order to evaluate the feasibility of the method for simultaneous analysis of Cr(VI) and Cr(III) in real matrices, the optimized analytical procedure was applied to analyze water and food samples. Firstly, the applicability of the calibration curves obtained with standard solutions was examined by constructing the matrix matched calibration curves for all real samples, separately. The linear ranges of these calibration curves were the same as those obtained for standard solutions. In addition, although, slope and intercept of these linear graphs showed acceptable consistency with those drawn using standard solutions, the matrix matched standard graphs were used to obtain the accurate recovery data. Analytical features of the matrix matched calibration curves are presented in Table S2. The applicability and reliability of the method were also examined by spiking the real samples with Cr(VI) and

Table 1 Recoveries and RSDs of chromium on three spiked standard levels (QC samples) in deionized water

Spiked Cr(VI) [a]	Found Cr(VI) [b]	Recovery [c]	RSD [d] Intra-day ($n = 5$)	Inter-day ($n = 3$)
0.25	0.26	104.0	7.5	8.5
1.00	0.99	99.0	5.8	7.0
25.00	25.65	102.6	3.6	4.1

[a] Spiked concentrations of Cr(VI) (μM)

[b] Recovered concentrations of Cr(VI) (μM) (n = 5)

[c] Recovery (%)

[d] Relative standard deviations (%)

Table 2 Comparison of the current method with the some reported methods for chromium speciation

Method	Matrices	LDR (μg L^{-1})	LOD [a] (μg L^{-1})	Extraction and separation procedure	Recovery (%)	References
ET-AAS [b]	Blood, serum and urine	0.03–4.4	0.005	IL-DLLBME [c]	94–104	[32]
ICP-MS	Tea leaves and infusion	0.1–100	0.007	SPE	96–105	[5]
ET-AAS	Water and urine	0.025–0.150	0.002	TCME [d]	90–102	[33]
FO-LADS [e]	Tap water and mineral waters	0.2–20	0.05	DLLME	95–101	[8]
FAAS [f]	Lake, tap and mineral waters	Blank-100	1.1	DMSPE [g] and CPE combination	91–103	[34]
Spectrofluorimetry	River, lake and sea waters	0.5–10	0.2	CPE	94–104	[17]
Spectrofluorimetry	Mineral and tap waters	100–10,000	50	Without extraction	95–100	[16]
Spectrofluorimetry	Natural water	5.2–104	0.44	Without extraction	98–103	[14]
Spectrofluorimetry	River and tap waters, garlic, onion and milk	0.52–5200	0.16	Without extraction	94–109	Present work

[a] LOD for Cr(VI)

[b] Electrothermal atomic absorption spectrometry

[c] Ionic liquid dispersive liquid–liquid bio-microextraction

[d] Temperature-controlled microextraction

[e] Fiber optic-linear array detection spectrophotometry

[f] Flame atomic absorption spectrometry

[g] Dispersive magnetic solid phase extraction

Cr(III) species. The concentrations of the spiked species were interpolated from their matrix matched calibration curves. The recoveries from spiked water and food real sample solutions containing low, middle and high concentrations of Cr(VI) and Cr(III) (0.1, 1.0 and 25.0 μM) are in the range of 93.9 to 109.4% (Table S3). All investigated real samples met the criteria for matrix effect (70 to 120%) according to the guidance document on analytical quality control and validation procedures for pesticide residues analysis in food and feed [35]. Furthermore, for elimination of the matrix effects, chromium content of water and food samples was obtained by using standard addition method. Therefore, the method can be applied successfully for various matrices with good accuracy.

Conclusion

A novel analytical method was developed for the speciation of Cr(III) and Cr(VI) ions using g-C_3N_4 NS as fluorescent probe without any previous pretreatment or separation steps and with spectrofluorimetric detection technique. The method is based on the quenching of the g-C_3N_4 NS fluorescence in the presence of Cr(VI). The probe showed some appealing features including compatibility with the green chemistry, low cost, high sensitivity, short analysis time and wide linear range. The dynamic linear range of the purposed method fulfill the requirements of World Health Organization (WHO) (<50 ppb ~ 0.96 μM) and Environmental Protection Agency (EPA) (<100 ppb ~1.92 μM)

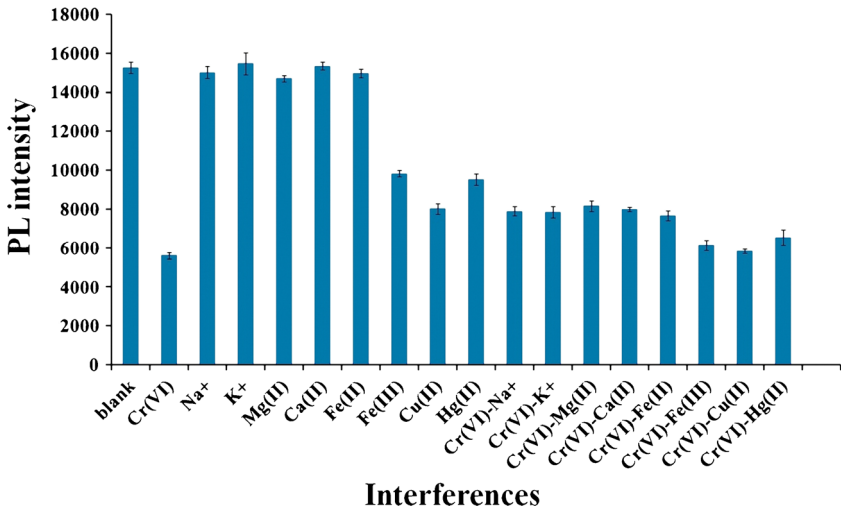

Fig. 4 The influence of some potentially interfering cations on the quenching ability of Cr(VI) using the optimized method (conditions: 10 mL of Cr(VI) solution, 50 μM; volume of g-C_3N_4 NS stock dispesion, 5 μL; reaction time, 5 min; concentration of the cations, 200 μM)

standards for total chromium in drinking water [34]. Based on the results, it believed that this study provides a promising florescence strategy for real environmental and food samples analysis with acceptable accuracy.

Acknowledgements The authors gratefully acknowledge the financial support provided by the Research Council of Ahvaz Jundishapur University of Medical Sciences and Nanotechnology Research Center under grant No. GP95134. This paper is extracted from Miss Salehnejad's thesis.

Compliance with ethical standards The author(s) declare that they have no competing interests.

References

1. Mathebula MW, Mandiwana K, Panichev N (2017) Speciation of chromium in bread and breakfast cereals. Food Chem 217:655–659
2. Devillers D, Buzier R, Simon S, Charriau A, Guibaud G (2016) Simultaneous measurement of Cr (III) and Cr (VI) in freshwaters with a single diffusive gradients in thin films device. Talanta 154: 533–538
3. Sumida T, Ikenoue T, Hamada K, Sabarudin A, Oshima M, Motomizu S (2005) On-line preconcentration using dual mini-columns for the speciation of chromium(III) and chromium(VI) and its application to water samples as studied by inductively coupled plasma-atomic emission spectrometry. Talanta 68:388–393
4. Chen S, Zhu L, Lu D, Cheng X, Zhou X (2010) Separation and chromium speciation by single-wall carbon nanotubes microcolumn and inductively coupled plasma mass spectrometry. Microchim Acta 169:123–128
5. Chen S, Zhu S, He Y, Lu D (2014) Speciation of chromium and its distribution in tea leaves and tea infusion using titanium dioxide nanotubes packed microcolumn coupled with inductively coupled plasma mass spectrometry. Food Chem 150:254–259
6. Chen Z, Megharaj M, Naidu R (2007) Speciation of chromium in waste water using ion chromatography inductively coupled plasma mass spectrometry. Talanta 72:394–400
7. Markiewicz B, Komorowicz I, Sajnog A, Belter M, Baralkiewicz D (2015) Chromium and its speciation in water samples by HPLC/ICP-MS-technique establishing metrological traceability: a review since 2000. Talanta 132:814–828
8. Yousefi SM, Shemirani F (2013) Selective and sensitive speciation analysis of Cr(VI) and Cr(III) in water samples by fiber optic-linear array detection spectrophotometry after ion pair based-surfactant assisted dispersive liquid–liquid microextraction. J Hazard Mater 254–255:134–140
9. Zeng C, Lin Y, Zhou N, Zheng J, Zhang W (2012) Room temperature ionic liquids enhanced the speciation of Cr(VI) and Cr(III) by hollow fiber liquid phase microextraction combined with flame atomic absorption spectrometry. J Hazard Mater 237–238:365–370
10. Moghadam MR, Dadfarnia S, Haji Shabani AM (2011) Speciation and determination of ultra-trace amounts of chromium by solidified floating organic drop microextraction (SFODME) and graphite furnace atomic absorption spectrometry. J Hazard Mater 186:169–174
11. Wang LL, Wang JQ, Zheng ZX, Xiao P (2010) Cloud point extraction combined with high-performance liquid chromatography for speciation of chromium(III) and chromium(VI) in environmental sediment samples. J Hazard Mater 177:114–118
12. Y-W W, Zhang J, Liu JF, Chen L, Deng ZL, Han MX, Wei XS, AM Y, Zhang HL (2012) Fe3O4@ZrO2 nanoparticles magnetic solid phase extraction coupled with flame atomic absorption spectrometry for chromium(III) speciation in environmental and biological samples. Appl Surf Sci 258:6772–6776
13. Cui H, He R, Wang J (2006) A simple and sensitive chromium speciation procedure by hyphenating flow injection on-line preconcentration with catalytic spectrophotometry. Talanta 70: 139–145
14. Hosseini MS, Belador F (2009) Cr(III)/Cr(VI) speciation determination of chromium in water samples by luminescence quenching of quercetin. J Hazard Mater 165:1062–1067
15. Kabasakalis V (1993) Fluorimetric Cr(VI) and Cr(III) speciation with crystal violet. Anal Lett 26:2269–2275
16. Paleologos EK, Lafis SI, Tzouwara-Karayanni SM, Karayannis MI (1998) Speciation analysis of CrIII–CrVI using flow injection analysis with fluorimetric detection. Analyst 123:1005–1009
17. Paleologos EK, Stalikas CD, Tzouwara-Karayanni SM, Karayannis MI (2001) Selective speciation of trace chromium through micelle-mediated preconcentration, coupled with micellar flow injection analysis–spectrofluorimetry. Anal Chim Acta 436:49–57
18. Carrasco PM, García I, Yate L, Zaera RT, Cabañero G, Grande HJ, Ruiz V (2016) Graphene quantum dot membranes as fluorescent sensing platforms for Cr (VI) detection. Carbon 109:658–665
19. Zhang JR, Zeng AL, Luo HQ, Li NB (2016) Fluorescent silver nanoclusters for ultrasensitive determination of chromium (VI) in aqueous solution. J Hazard Mater 304:66–72
20. Liu X, Li T, Wu Q, Yan X, Wu C, Chen X, Zhang G (2017) Carbon nanodots as a fluorescence sensor for rapid and sensitive detection of Cr (VI) and their multifunctional applications. Talanta 165:216–222
21. Han Q, Wang B, Gao J, Cheng Z, Zhao Y, Zhang Z, Qu L (2016) Atomically thin Mesoporous Nanomesh of graphitic C3N4for high-efficiency Photocatalytic hydrogen evolution. ACS Nano 10:2745–2751
22. Zhou Z, Shen Y, Li Y, Liu A, Liu S, Zhang Y (2015) Chemical cleavage of layered carbon nitride with enhanced photoluminescent performances and photoconduction. ACS Nano 9:12480–12487
23. Guo X, Wang Y, Wu F, Ni Y, Kokot S (2015) Preparation of protonated, two-dimensional graphitic carbon nitride nanosheets by exfoliation, and their application as a fluorescent probe for trace analysis of copper(II). Microchim Acta 183:773–780
24. Rong M, Lin L, Song X, Wang Y, Zhong Y, Yan J, Feng Y, Zeng X, Chen X (2015) Fluorescence sensing of chromium (VI) and ascorbic acid using graphitic carbon nitride nanosheets as a fluorescent "switch". Biosens Bioelectron 68:210–217
25. Chen HY, Ruan LW, Jiang X, Qiu LG (2015) Trace detection of nitro aromatic explosives by highly fluorescent g-C3N4 nanosheets. Analyst 140:637–643
26. Han J, Zou HY, Gao MX, Huang CZ (2016) A graphitic carbon nitride based fluorescence resonance energy transfer detection of riboflavin. Talanta 148:279–284
27. Hu K, Zhong T, Huang Y, Chen Z, Zhao S (2014) Graphitic carbon nitride nanosheet-based multicolour fluorescent nanoprobe for multiplexed analysis of DNA. Microchim Acta 182:949–955
28. Salehnia F, Hosseini M, Ganjali MR (2017) A fluorometric aptamer based assay for cytochrome C using fluorescent graphitic carbon nitride nanosheets. Microchim Acta 184:2157–2163
29. Zhang Y, Pan Q, Chai G, Liang M, Dong G, Zhang Q, Qiu j (2013) Synthesis and luminescence mechanism of multicolor-emitting g-C3N4 Nanopowders by low temperature thermal condensation of melamine. Sci Rep 3:1943
30. Lee EZ, Jun YS, Hong WH, Thomas A, Jin MM (2010) Cubic mesoporous graphitic carbon(IV) nitride: an all-in-one chemosensor for selective optical sensing of metal ions. Angew Chem Int Ed 49:9706–9710
31. Rong M, Lin L, Song X, Zhao T, Zhong Y, Yan J, Wang Y, Chen X (2015) A label-free fluorescence sensing approach for selective and sensitive detection of 2,4,6-Trinitrophenol (TNP) in aqueous

solution using graphitic carbon nitride nanosheets. Anal Chem 87: 1288–1296

32. Shirkhanloo H, Ghazaghi M, Mousavi HZ (2016) Chromium speciation in human blood samples based on acetyl cysteine by dispersive liquid-liquid biomicroextraction and in-vitro evaluation of acetyl cysteine/cysteine for decreasing of hexavalent chromium concentration. J Pharm Biomed Anal 118:1–8
33. Sadeghi S, Zeraatkar Moghaddam A (2012) Preconcentration and speciation of trace amounts of chromium in saline samples using temperature-controlled microextraction based on ionic liquid as extraction solvent and determination by electrothermal atomic absorption spectrometry. Talanta 99:758–766
34. Diniz KM, Tarley CRT (2015) Speciation analysis of chromium in water samples through sequential combination of dispersive magnetic solid phase extraction using mesoporous amino-functionalized Fe_3O_4/SiO_2 nanoparticles and cloud point extraction. Microchem J 123:185–195
35. Zare M, Ramezani Z, Rahbar N (2016) Development of zirconia nanoparticles-decorated calcium alginate hydrogel fibers for extraction of organophosphorous pesticides from water and juice samples: facile synthesis and application with elimination of matrix effects. J Chromatogr A 1473:28–37